PARAMETER RECOVERY FOR THE 2 DIMENSIONAL NAVIER–STOKES EQUATIONS VIA CONTINUOUS DATA ASSIMILATION*

ELIZABETH CARLSON[†], JOSHUA HUDSON[‡], AND ADAM LARIOS[§]

Abstract. We study a continuous data assimilation algorithm proposed by Azouani, Olson, and Titi (AOT) in the context of an unknown viscosity. We determine the large-time error between the true solution of the 2 dimensional Navier–Stokes equations and the assimilated solution due to discrepancy between an approximate viscosity and the physical viscosity. Additionally, we develop an algorithm that can be run in tandem with the AOT algorithm to recover both the true solution and the true viscosity using only spatially discrete velocity measurements.

Key words. parameter recovery, continuous data assimilation, Navier–Stokes equations, Reynolds number, viscosity, approximation

AMS subject classifications. 34D06, 35Q30, 35Q35, 37C50

DOI. 10.1137/19M1248583

1. Introduction. A major difficulty in performing accurate, practical simulations of dynamical systems is that one typically does not have complete information about the initial state of the system, nor the exact physical parameters of the system, which may be inaccurately measured, or simply unknown. In this paper, we present an algorithm based on data assimilation that addresses both of these difficulties. The term data assimilation refers to a wide class of techniques for incorporating observational data into simulations to increase their accuracy. It is especially relevant for situations in which information about the initial data is sparse. Recently, in a paper by Azouani, Olson, and Titi (AOT) [4], a new approach to data assimilation, which we refer to as the AOT algorithm, was proposed. This algorithm uses a feedback control term at the PDE level to penalize deviations from the observed data. In the present work, we apply the AOT algorithm in the setting of an unknown diffusion coefficient (e.g., viscosity or Reynolds number) and propose an algorithm which changes the diffusion coefficient dynamically as the simulation evolves in time, driving the parameter to its true value.

We demonstrate this parameter recovery method for estimating viscosity using the feedback control method of data assimilation proposed in [4], which states that

^{*}Submitted to the journal's Methods and Algorithms for Scientific Computing section March 7, 2019; accepted for publication (in revised form) October 29, 2019; published electronically January 14, 2020.

 $[\]rm https://doi.org/10.1137/19M1248583$

Funding: The work of the first author was partially supported by NSF GRFP grant 1610400. The work of the second author was partially supported by NSF grant DMS-1517027. The work of the third author was partially supported by NSF grant DMS-1716801. Computational resources were provided by Lilly Endowment, Inc., through its support for the Indiana University Pervasive Technology Institute, and in part by the Indiana METACyt Initiative. The Indiana METACyt Initiative at IU was also supported in part by Lilly Endowment, Inc.

[†]Department of Mathematics, University of Nebraska–Lincoln, Lincoln, NE 68588-0130 (elizabeth. carlson@huskers.unl.edu).

[‡]University of Maryland, Baltimore County, 1000 Hilltop Circle, Baltimore, MD 21055. Current address: Johns Hopkins University Applied Physics Laboratory, 11100 Johns Hopkins Road, Laurel, MD 20723-6099 (Joshua.Hudson@jhuapl.edu).

 $[\]ensuremath{^\S{}} \text{Department}$ of Mathematics, University of Nebraska–Lincoln, Lincoln, NE 68588-0130 (alarios@unl.edu).

given a dissipative dynamical system (of possibly infinite dimension) of the form

$$\frac{d\mathbf{u}}{dt} = F(\mathbf{u})$$

with missing initial data, we can instead solve the system,

$$\frac{d\mathbf{v}}{dt} = F(\mathbf{v}) + \mu(I_h(\mathbf{u}) - I_h(\mathbf{v})),$$

$$\mathbf{v}(0) = \mathbf{v}_0,$$

where μ is a sufficiently large positive relaxation parameter, $I_h(\mathbf{u})$ represents the observational measurements, and \mathbf{v}_0 is arbitrarily chosen in a suitable function space. The function I_h is a straightforward interpolant satisfying particular bounds (stated in the preliminaries), and is often taken to be modal projection.

Following the analysis of [4] on the 2 dimensional (2D) incompressible Navier–Stokes equations, analytical bounds on the large time error of \mathbf{v} with respect to the true solution \mathbf{u} are shown to be directly dependent upon the difference between our chosen viscosity and the true viscosity. Computationally, it is observed that the term involving the error of the viscosities closely matches the error between the solutions \mathbf{v} and \mathbf{u} . Using this fact, we develop a heuristic algorithm for computationally recovering the true viscosity and simultaneously converge to the true solution \mathbf{u} .

Our error estimates in this work are also relevant to the setting of subgrid scale data. In real-world settings, simulations are often underresolved; in particular, it is not always possible to run simulations with the physical viscosity (see, e.g., [47, 55, 5] and the references therein). The error estimates we prove in this paper indicate that one may simulate flows using the AOT algorithm with a viscosity which is, e.g., larger than the true viscosity, and be assured that deviations from the true solution are controlled (in the L^2 and H^1 norms) by the difference in the viscosities.

We note that classical data assimilation is largely focused on statistical optimization approaches utilizing the Kalman filter [38] or 3/4 dimensional-Var methods, and variations of these techniques (see, e.g., [15, 39, 45, 48], and the references therein). The AOT algorithm (which is also called continuous data assimilation or CDA in the literature), differs markedly from the Kalman filter approach. Instead of employing statistical tools at the numerical level, AOT data assimilation arises at the PDE level via a feedback-control term which penalizes deviations from interpolations of observable data. This interpolation is a key difference between the AOT method and the so-called nudging or Newtonian relaxation methods introduced in [3, 31], as it allows for significantly more sparse initial data. For an overview of nudging methods, see, e.g., [40]. We mention that a method that shares some features with the AOT algorithm was introduced in [9] in the context of stochastic differential equations. The AOT algorithm and its extensions have been the subject of much recent theoretical work; see, e.g., [1, 6, 7, 8, 13, 20, 21, 22, 23, 24, 26, 27, 28, 30, 33, 34, 35, 36, 41, 50, 51, 52, 53]. Computational trials of the AOT algorithm and its variants were carried out on a wide variety of equations in several recent works, including [2, 16, 46, 29, 42, 43, 44, 17, 49, 58]. We also mention an upcoming work [18], currently a preprint, which explores some similar ideas contained in this paper in the context of continuous data assimilation for the Rayleigh-Bénard convection equations with unknown Prandtl number, although parameter recovery is not explored in that work.

The paper is organized as follows: in section 2, we describe the mathematical framework for the problems we consider. In section 3 we consider the AOT data

assimilation algorithm and show that with only an approximation of the true viscosity, the reference solution can still be recovered using data assimilation. We analyze the Navier–Stokes equations with periodic boundary conditions, but our techniques can be extended to other boundary conditions and other dissipative systems. We also provide computational evidence that illustrates the effectiveness of the AOT algorithm in the setting of a mismatched viscosity parameter, as well as the practical performance one might expect in a typical flow. In section 5, motivated by our rigorous results, we consider the problem of parameter recovery and propose two algorithms to recover the true viscosity "on-the-fly" (i.e., during the simulation) using only the AOT algorithm and the observational data. In our computational experiments, we observe that the convergence to the true viscosity and the true solution happen exponentially fast in time.

2. Preliminaries. In this section, we state the theorems and other preliminaries needed to solve the 2D incompressible Navier–Stokes equations and the associated modified equations utilizing the AOT algorithm [4]. The statements given in the section without proof are standard, and proofs can be found, e.g., in [14, 25, 54, 57, 56]. We consider the 2D incompressible Navier–Stokes equations in dimensionless form on a spatial domain Ω ,

(2.1a)
$$\partial_t \mathbf{u} + (\mathbf{u} \cdot \nabla) \mathbf{u} = -\nabla p + \nu_1 \Delta \mathbf{u} + \mathbf{f} \quad \text{in } \Omega \times [0, T],$$

(2.1b)
$$\nabla \cdot \mathbf{u} = 0 \qquad \text{in } \Omega \times [0, T],$$

(2.1c)
$$\mathbf{u}(\mathbf{x},0) = \mathbf{u}_0(\mathbf{x}) \quad \text{in } \Omega,$$

where $\nu_1 > 0$ is the kinematic viscosity.

We take the spatial domain, Ω , to be the torus, i.e., $\Omega = \mathbb{T}^2 = \mathbb{R}^2/\mathbb{Z}^2$, which is an open, bounded, and connected domain. As is customary, we define the space

$$\mathcal{V} := \left\{ \mathbf{w} : \mathbb{T}^2 \to \mathbb{R}^2 \mid \mathbf{w} \in C^{\infty}(\mathbb{T}^2), \nabla \cdot \mathbf{w} = 0, \int_{\mathbb{T}^2} \mathbf{w}(\mathbf{x}) \, d\mathbf{x} = \mathbf{0} \right\}$$

and, subsequently, the spaces $H:=\overline{\mathcal{V}}$ in $L^2(\Omega;\mathbb{R}^2)$ and $V:=\overline{\mathcal{V}}$ in $H^1(\Omega;\mathbb{R}^2)$. H and V are subspaces of $L^2(\Omega;\mathbb{R}^2)$ and $H^1(\Omega;\mathbb{R}^2)$, respectively, and hence are Hilbert spaces with the inner products defined as

$$(\mathbf{u}, \mathbf{v}) = \int_{\mathbb{T}^2} \mathbf{u} \cdot \mathbf{v} \, d\mathbf{x}, \qquad ((\mathbf{u}, \mathbf{v})) = \sum_{i,j=1}^2 \int_{\mathbb{T}^2} \frac{\partial u_i}{\partial x_j} \frac{\partial v_i}{\partial x_j} \, d\mathbf{x}$$

with corresponding norms $|\mathbf{u}| = \sqrt{(\mathbf{u}, \mathbf{u})}$ and $\|\mathbf{u}\| = \sqrt{((\mathbf{u}, \mathbf{u}))}$.

We denote the Leray projection $P_{\sigma}: L^2(\Omega) \to H$ defined by $P_{\sigma}\mathbf{u} = \mathbf{u} - \nabla \triangle^{-1}(\nabla \cdot \mathbf{u})$ (see, e.g., [14, 25, 54, 57, 56]). We can equivalently consider (2.1), where P_{σ} is the orthogonal projection of a vector field onto its divergence-free part. As in [4], we define the Stokes operator A and the bilinear term $B: V \times V \to V^*$ as the continuous extensions of the operators A and B defined on $V \times V$ as

$$A\mathbf{u} = -P_{\sigma} \triangle \mathbf{u}$$
 and $B(\mathbf{u}, \mathbf{v}) = P_{\sigma}(\mathbf{u} \cdot \nabla \mathbf{v}),$

and we define the domain of A to be $\mathcal{D}(A) := \{\mathbf{u} \in V : A\mathbf{u} \in H\}$. Also note that A is a linear self-adjoint and positive definite operator with a compact inverse, so there exists a complete orthonormal set of eigenfunctions \mathbf{w}_i in H such that $A\mathbf{w}_i = \lambda_i \mathbf{w}_i$

with the eigenvalues strictly positive and monotonically increasing. Furthermore, the following Poincaré inequalities hold:

$$\lambda_1 \|\mathbf{u}\|_{L^2}^2 \le \|\nabla \mathbf{u}\|_{L^2}^2 \quad \text{for} \quad \mathbf{u} \in V,$$

$$\lambda_1 \|\nabla \mathbf{u}\|_{L^2}^2 \le \|A\mathbf{u}\|_{L^2}^2 \quad \text{for} \quad \mathbf{u} \in D(A),$$

where $\lambda_1 = 4\pi^2$ is the first eigenvalue of the Stokes operator. Thus, $|\nabla \mathbf{u}|$ and $||\mathbf{u}||$ are equivalent norms on V. In 2 dimensions, the following Brezis-Gallouet inequality [10], also holds for all $\mathbf{u} \in \mathcal{D}(A)$:

(2.2)
$$\|\mathbf{u}\|_{L^{\infty}} \le c \|\mathbf{u}\| \left\{ 1 + \log \frac{|A\mathbf{u}|^2}{4\pi^2 \|\mathbf{u}\|^2} \right\}.$$

We note that the bilinear operator, B, has the property

(2.3)
$$\langle B(\mathbf{u}, \mathbf{v}), \mathbf{w} \rangle = -\langle B(\mathbf{u}, \mathbf{w}), \mathbf{v} \rangle$$

for all $\mathbf{u}, \mathbf{v}, \mathbf{w} \in V$. This implies B also satisfies

$$\langle B(\mathbf{u}, \mathbf{w}), \mathbf{w} \rangle = 0$$

for all $\mathbf{u}, \mathbf{v}, \mathbf{w} \in V$. Moreover, the following inequalities hold:

(2.5)
$$|\langle B(\mathbf{u}, \mathbf{v}), \mathbf{w} \rangle| \leq ||\mathbf{u}||_{L^{\infty}(\Omega)} ||\mathbf{v}|| ||\mathbf{w}| \qquad \text{for } \mathbf{u} \in L^{\infty}(\Omega), \mathbf{v} \in V, \mathbf{w} \in H,$$
(2.6)
$$|\langle B(\mathbf{u}, \mathbf{v}), \mathbf{w} \rangle| \leq c |\mathbf{u}|^{1/2} ||\mathbf{u}||^{1/2} ||\mathbf{v}|| ||\mathbf{w}||^{1/2} ||\mathbf{w}||^{1/2} \qquad \text{for } \mathbf{u}, \mathbf{v}, \mathbf{w} \in V,$$

$$|(B(\mathbf{u}, \mathbf{v}), \mathbf{w})| \le c|\mathbf{u}|^{1/2}|A\mathbf{u}|^{1/2}||\mathbf{v}|||\mathbf{w}| \qquad \text{for } \mathbf{u} \in \mathcal{D}(A), \mathbf{v} \in V, \mathbf{w} \in H.$$

Due to the periodic boundary conditions, it also holds (in 2 dimensions) that

(2.9)
$$(B(\mathbf{w}, \mathbf{w}), A\mathbf{w}) = 0$$
 for every $\mathbf{w} \in \mathcal{D}(A)$.

Therefore, for $\mathbf{u}, \mathbf{w} \in \mathcal{D}(A)$,

(2.10)
$$(B(\mathbf{u}, \mathbf{w}), A\mathbf{w}) + (B(\mathbf{w}, \mathbf{u}), A\mathbf{w}) = -(B(\mathbf{w}, \mathbf{w}), A\mathbf{u}).$$

Without loss of generality, we will assume $\mathbf{f} \in L^{\infty}(0,T;H)$ so that $P_{\sigma}f = f$. Thus, we may rewrite (2.1) as

(2.11a)
$$\frac{d}{dt}\mathbf{u} + B(\mathbf{u}, \mathbf{u}) + \nu_1 A \mathbf{u} = \mathbf{f} \qquad \text{in } \Omega \times [0, T].$$

(2.11b)
$$\mathbf{u}(\mathbf{x},0) = \mathbf{u}_0(\mathbf{x}) \quad \text{in } \Omega$$

The pressure term can be recovered using de Rham's theorem [57, 25], a corollary of which is that

(2.12)
$$\mathbf{g} = \nabla p$$
 with p a distribution if and only if $\langle \mathbf{g}, \mathbf{h} \rangle = 0$ for all $\mathbf{h} \in \mathcal{V}$.

For a given force f and some initial data \mathbf{u}_0 , it is classical that a unique global solution \mathbf{u} of (2.11) will exist. However, we don't expect to know \mathbf{u}_0 exactly, and so cannot compute $\mathbf{u}(t)$ from (2.11); rather, we consider the case that measurement data is collected on $\mathbf{u}(t)$ over the time interval [0,T], sufficient for the interpolation operator I_h to construct the interpolation $I_h(\mathbf{u}(t))$ on [0,T]. From here, we can define a new system, dubbed the data assimilation system, by introducing a feedback control (nudging term) via I_h into (2.11) (or (2.1)), as is done in [4].

We will construct our data assimilation system under the more general case of having only an approximate viscosity, ν_2 :

(2.13a)
$$\frac{d}{dt}\mathbf{v} + B(\mathbf{v}, \mathbf{v}) + \nu_2 A\mathbf{v} = \mathbf{f} + \mu P_{\sigma}(I_h(\mathbf{u}) - I_h(\mathbf{v})),$$

$$\mathbf{v}(\mathbf{x},0) = \mathbf{v}_0(\mathbf{x}).$$

Here, $\mu > 0$ is a relaxation parameter, ν_2 a kinematic viscosity approximating ν_1 , and I_h is a linear interpolant satisfying

(2.14)
$$\|\varphi - I_h(\varphi)\|_{L^2(\Omega)}^2 \le c_0 h^2 \|\varphi\|_{H^1(\Omega)}^2.$$

From [4], (2.13) has a unique solution given either no-slip Dirichlet or periodic boundary conditions as stated in the following theorem.

THEOREM 2.1. Suppose I_h satisfies (2.14) and $\mu c_0 h^2 \leq \nu_2$, where c_0 is the constant from (2.14). Then the CDA equations (2.13) possess unique strong solutions that satisfy

(2.15)
$$\mathbf{v} \in C([0,T];V) \cap L^2((0,T);D(A)) \text{ and } \frac{d\mathbf{v}}{dt} \in L^2((0,T);H)$$

for any T > 0. Furthermore, this solution is in C([0,T],V) and depends continuously on the initial data \mathbf{v}_0 in the V norm.

For (2.11) and (2.13), we denote the dimensionless Grashof numbers as

(2.16)
$$G_1 = \frac{1}{\lambda_1 \nu_1^2} \limsup_{t \to \infty} \|\mathbf{f}(t)\|_{L^2(\Omega)},$$

(2.17)
$$G_2 = \frac{1}{\lambda_1 \nu_2^2} \limsup_{t \to \infty} \|\mathbf{f}(t)\|_{L^2(\Omega)}.$$

In 2 dimensions, it is classical that (2.1) possesses a unique global strong solution. Furthermore, we have explicit upper bounds on the norms of the solutions in H and V in terms of G_1 .

THEOREM 2.2. Fix T > 0. Suppose that \mathbf{u} is a solution of (2.11), corresponding to the initial value $\mathbf{u}_0 \in V$. Then there exists a time t_0 which depends on \mathbf{u}_0 such that for all $t \geq t_0$, it holds that

$$(2.18) |\mathbf{u}(t)|^2 \le 2\nu_1^2 G_1^2 and \int_t^{t+T} \|\mathbf{u}(\tau)\|^2 d\tau \le 2\left(1 + T\lambda_1\nu_1\right)\nu_1 G_1^2.$$

In the case of periodic boundary conditions it also holds for all $t \geq t_0$ that

(2.19)
$$\|\mathbf{u}(t)\|^{2} \leq 2\lambda_{1}\nu_{1}^{2}G_{1}^{2}, \qquad \int_{t}^{t+T} |A\mathbf{u}(\tau)|^{2} d\tau \leq 2\left(1 + T\lambda_{1}\nu_{1}\right)\lambda_{1}\nu_{1}G_{1}^{2}.$$

Furthermore, if $\mathbf{f} \in H$ is time independent then

$$(2.20) |A\mathbf{u}(t)|^2 \le c\lambda_1^2\nu_1^2(1+G_1)^4.$$

To prove our main theoretical results, we will need the following corollary of the statement of the uniform Grönwall lemma proved in [37].

LEMMA 2.3 (generalized uniform Grönwall inequality). Let α be a locally integrable real-valued function defined on $(0,\infty)$, satisfying the following conditions for some $0 < T < \infty$:

$$\liminf_{t \to \infty} \int_{t}^{t+T} \alpha(\tau) d\tau = \gamma > 0,$$

$$\limsup_{t \to \infty} \int_{t}^{t+T} \alpha^{-}(\tau) d\tau = \Gamma < \infty,$$

where $\alpha^- = \max\{-\alpha, 0\}$. Furthermore, let β be a real-valued locally integrable function defined on $(0, \infty)$, and let $\beta^+ = \max\{\beta, 0\}$. Suppose that ξ is an absolutely continuous nonnegative function on $(0, \infty)$ such that

(2.21)
$$\frac{d}{dt}\xi + \alpha\xi \le \beta \qquad a.e. \ on \ (0, \infty).$$

Then

$$\xi(t) \le \xi(t_0) \Gamma' e^{-\frac{\gamma}{2T}(t-t_0)} + \left(\sup_{t \ge t_0} \int_t^{t+T} \beta^+(\tau) \ d\tau \right) \Gamma' \frac{e^{\gamma/2}}{e-1},$$

where $\Gamma' = e^{\Gamma + 1 + \gamma/2}$ and t_0 is chosen sufficiently large so that, for all $s \geq t_0$,

(2.22)
$$\int_{s}^{s+T} \alpha^{-}(\sigma) d\sigma \leq \Gamma + 1$$

and

(2.23)
$$\int_{0}^{s+T} \alpha(\sigma) \ d\sigma \ge \gamma/2.$$

We will also make use of the following lemma proved in [4].

LEMMA 2.4. Let
$$\phi(r) = r - \beta(1 + \log r)$$
, where $\beta > 0$. Then

$$\min\{\phi(r): r > 1\} > -\beta \log \beta.$$

3. Error of CDA to viscosity. We now present our first result. In [4], it was shown for the case $\nu_1 = \nu_2$, that given a strong solution \mathbf{u} of (2.1) and an interpolant I_h satisfying (2.14), for sufficiently large μ and sufficiently small h, the corresponding solution \mathbf{v} of (2.13) will converge in the L^2 sense to \mathbf{u} exponentially fast in time for any $\mathbf{v}_0 \in V$ (and convergence in the H^1 sense under stronger smoothness assumptions). We extend this result to include the case $\nu_1 \neq \nu_2$. In particular, we show that the L^2 error decays exponentially in time, down to a level which is controlled by the difference in the viscosities. Moreover, this level goes to zero as $\nu_2 \to \nu_1$. This means that the AOT algorithm for 2D Navier–Stokes can recover the solution approximately even when the true viscosity is unknown, and that the accuracy improves as the approximation of the viscosity improves, and with the same order.

THEOREM 3.1. Let \mathbf{u} and \mathbf{v} be solutions to the systems (2.11) and (2.13), respectively, with initial data \mathbf{u}_0 , $\mathbf{v}_0 \in V$. Suppose ν_1 , $\nu_2 > 0$. Let $\mu \geq 20\pi^2 c^2 \frac{\nu_1^2}{\nu_2} G_1^2$ and $h \leq (\frac{1}{40\pi^2 c^2 c_0 G_1^2} \frac{\nu_2^2}{\nu_1^2})^{1/2}$. Then for any T such that $\frac{1}{4\pi^2 \nu_1} < T < \infty$, and for a.e. t > T, it holds that

$$|\mathbf{u}(t) - \mathbf{v}(t)|^2 \le |\mathbf{u}(t_0) - \mathbf{v}(t_0)|^2 e^{1+\gamma/2} e^{-\frac{\gamma}{2T}(t-t_0)} + C \cdot \frac{(\nu_2 - \nu_1)^2}{\nu_2},$$

where

$$C := \frac{e^{1+\gamma}}{e-1} (2(1+4\pi^2 T \nu_1)\nu_1 G_1^2)$$

and

$$\gamma := \liminf_{t \to \infty} \int_t^{t+T} \mu - \frac{2c^2}{\nu_2} \|\mathbf{u}(s)\|^2 ds > 0.$$

In particular,

$$\limsup_{t \to \infty} |\mathbf{u}(t) - \mathbf{v}(t)| \le C \frac{|\nu_2 - \nu_1|}{\sqrt{\nu_2}}.$$

The idea of the proof is similar to the proof of the corresponding result in [4], except that we have an additional term to handle since we allow for the case $\nu_1 \neq \nu_2$.

Proof. We denote $\mathbf{w} := \mathbf{u} - \mathbf{v}$, and subtract (2.13a) from (2.11a) to obtain

$$\mathbf{w}_t + B(\mathbf{w}, \mathbf{u}) + B(\mathbf{v}, \mathbf{w}) = -\nu_1 A \mathbf{u} + \nu_2 A \mathbf{v} - \mu P_{\sigma}(I_h(\mathbf{w})),$$

which can be simplified to

(3.1)
$$\mathbf{w}_t + B(\mathbf{w}, \mathbf{u}) + B(\mathbf{v}, \mathbf{w}) = (\nu_2 - \nu_1)A\mathbf{u} - \nu_2 A\mathbf{w} - \mu P_{\sigma}(I_h(\mathbf{w}))$$

with initial data given by

$$\mathbf{w}(\mathbf{x},0) = \mathbf{w}_0(\mathbf{x}) := \mathbf{u}_0(x) - \mathbf{v}_0(x).$$

We take the action of (3.1) on \mathbf{w} , and utilize the Cauchy–Schwarz and Young's inequalities to obtain

$$\frac{1}{2} \frac{d}{dt} |\mathbf{w}|^2 + \nu_2 ||\mathbf{w}||^2
= (\nu_2 - \nu_1)((\mathbf{u}, \mathbf{w})) - \langle B(\mathbf{w}, \mathbf{u}), \mathbf{w} \rangle - \mu(P_{\sigma}(I_h(\mathbf{w})), \mathbf{w})
\leq |\nu_2 - \nu_1| ||\mathbf{u}|| ||\mathbf{w}||
- \langle B(\mathbf{w}, \mathbf{u}), \mathbf{w} \rangle - \mu(P_{\sigma}(I_h(\mathbf{w})), \mathbf{w})
\leq \frac{|\nu_2 - \nu_1|^2}{2\nu_2} ||\mathbf{u}||^2 + \frac{\nu_2}{2} ||\mathbf{w}||^2
- \langle B(\mathbf{w}, \mathbf{u}), \mathbf{w} \rangle - \mu(P_{\sigma}(I_h(\mathbf{w})), \mathbf{w}).$$

Using (2.6), (2.14), and Young's inequality, we obtain

$$\begin{split} &\frac{1}{2} \frac{d}{dt} |\mathbf{w}|^2 + \frac{\nu_2}{2} ||\mathbf{w}||^2 \\ &\leq -\langle B(\mathbf{w}, \mathbf{u}), \mathbf{w} \rangle + \frac{|\nu_2 - \nu_1|^2}{2\nu_2} ||\mathbf{u}||^2 - \mu(P_{\sigma}(I_h(\mathbf{w})), \mathbf{w}) \\ &\leq c ||\mathbf{w}|| ||\mathbf{w}|| ||\mathbf{u}|| + \frac{(\nu_2 - \nu_1)^2}{2\nu_2} ||\mathbf{u}||^2 \\ &- \mu(P_{\sigma}(I_h(\mathbf{w}) - \mathbf{w}), \mathbf{w}) - \mu ||\mathbf{w}||^2 \\ &\leq c ||\mathbf{w}|| ||\mathbf{w}|| ||\mathbf{u}|| + \frac{(\nu_2 - \nu_1)^2}{2\nu_2} ||\mathbf{u}||^2 \\ &+ \mu \sqrt{c_0 h^2} ||\mathbf{w}|| ||\mathbf{w}|| - \mu ||\mathbf{w}||^2 \\ &\leq \frac{c^2}{\nu_2} ||\mathbf{w}||^2 ||\mathbf{u}||^2 + \frac{\nu_2}{4} ||\mathbf{w}||^2 \\ &+ \frac{(\nu_2 - \nu_1)^2}{2\nu_2} ||\mathbf{u}||^2 + \mu \sqrt{c_0 h^2} ||\mathbf{w}|| ||\mathbf{w}|| - \mu ||\mathbf{w}||^2 \\ &\leq \frac{c^2}{\nu_2} ||\mathbf{w}||^2 ||\mathbf{u}||^2 + \frac{\nu_2}{4} ||\mathbf{w}||^2 \\ &+ \frac{(\nu_2 - \nu_1)^2}{2\nu_2} ||\mathbf{u}||^2 + \frac{\mu c_0 h^2}{2} ||\mathbf{w}||^2 - \frac{\mu}{2} ||\mathbf{w}||^2. \end{split}$$

This implies

(3.2)
$$\frac{1}{2} \frac{d}{dt} |\mathbf{w}|^2 + \left(\frac{\nu_2}{4} - \frac{\mu c_0 h^2}{2}\right) ||\mathbf{w}||^2 + \left(\frac{\mu}{2} - \frac{c^2}{\nu_2} ||\mathbf{u}||^2\right) ||\mathbf{w}||^2$$
$$\leq \frac{(\nu_2 - \nu_1)^2}{2\nu_2} ||\mathbf{u}||^2.$$

Since, by assumption,

$$\mu \geq 20\pi^2 c^2 \frac{\nu_1^2}{\nu_2} G_1^2$$

and

$$h \le \left(\frac{1}{40c^2c_0\pi^2G_1^2}\frac{\nu_2^2}{\nu_1^2}\right)^{1/2},$$

it follows that

(3.3)
$$\frac{1}{2}\frac{d}{dt}|\mathbf{w}|^2 + \left(\frac{\mu}{2} - \frac{c^2}{\nu_2}\|\mathbf{u}\|^2\right)|\mathbf{w}|^2 \le \frac{(\nu_2 - \nu_1)^2}{2\nu_2}\|\mathbf{u}\|^2.$$

Hence, we have an inequality of the form (2.21). Fix T>0 such that $\frac{1}{4\pi^2\nu_1}< T<\infty$. Then

$$\liminf_{t \to \infty} \int_{t}^{t+T} \mu - \frac{2c^{2}}{\nu_{2}} \|\mathbf{u}(s)\|^{2} ds$$

$$\geq T\mu - \frac{2c^{2}}{\nu_{2}} (2(1 + 4\pi^{2}T\nu_{1})\nu_{1}G_{1}^{2})) > 0,$$

thanks to the assumption $\mu \geq 20\pi^2 c^2 \frac{\nu_1^2}{\nu_2} G_1^2$. Define

$$\gamma := \liminf_{t \to \infty} \int_t^{t+T} \mu - \frac{2c^2}{\nu_2} ||\mathbf{u}(s)||^2 ds > 0.$$

Choose t_0 sufficiently large so that Theorem 2.2 holds and the inequalities (2.22) and (2.23) hold. Then

$$\Gamma := \limsup_{t \to \infty} \int_t^{t+T} \alpha^-(\tau) \ d\tau = 0 < \infty,$$

and we can apply Lemma 2.3 to conclude that, for a.e. $t > t_0$,

$$\begin{aligned} &|\mathbf{w}(t)|^{2} \\ &\leq |\mathbf{w}(t_{0})|^{2} e^{1+\gamma/2} e^{-\frac{\gamma}{2T}(t-t_{0})} + \left(\sup_{t \geq t_{0}} \int_{t}^{t+T} \frac{(\nu_{2} - \nu_{1})^{2}}{\nu_{2}} ||\mathbf{u}(\tau)||^{2} d\tau \right) \frac{e^{1+\gamma}}{e-1} \\ &\leq |\mathbf{w}(t_{0})|^{2} e^{1+\gamma/2} e^{-\frac{\gamma}{2T}(t-t_{0})} + C \cdot \frac{(\nu_{2} - \nu_{1})^{2}}{\nu_{2}}, \end{aligned}$$

where $C := \frac{e^{1+\gamma}}{e-1}(2(1+4\pi^2T\nu_1)\nu_1G_1^2)$. Taking the limit supremum as $t\to 0$ establishes the result.

We now prove a similar result for the H^1 norm of the difference of the solutions, the proof of which closely follows that of [4], although again with an additional term to allow for $\nu_1 \neq \nu_2$.

Theorem 3.2. Given the systems (2.11) and (2.13) with periodic boundary conditions, and given $\mu \geq 12\pi^2\nu_1 JG_1$, with

$$J := \left[2c \log \left(\frac{2c^{3/2}\nu_1}{\nu_2} \right) + 4c \log(1 + G_1) \right],$$

and $\mu c_0 h^2 \leq \nu_2$ (or, more universally, $h < \sqrt{\frac{\nu_2}{12\pi^2 c_0 \nu_1 JG}}$), then with the following constants:

- $C := 32\pi^2 \nu_1 G_1^2 \Gamma' \frac{e^{\gamma/2}}{e-1}$
- $\gamma := \liminf_{t \to \infty} \int_t^{t+T} \frac{1}{2} \left[\mu \frac{J^2}{\mu} |A\mathbf{u}|^2 \right] d\tau$,
- $\bullet \ \Gamma := \limsup_{t \to \infty} \int_t^{t+T} \max \left\{ \tfrac{1}{2} \left[\mu \frac{\tilde{J^2}}{\mu} |A\mathbf{u}|^2 \right], 0 \right\} d\tau,$
- $\Gamma' := e^{\Gamma + 1 + \gamma/2}$

and for any $T \geq 4\pi^2 \nu_1$, we obtain

$$\|\mathbf{u}(t) - \mathbf{v}(t)\|^2 \le \|\mathbf{u}(0) - \mathbf{v}(0)\|^2 \Gamma' e^{-\frac{\gamma}{2T}(t-t_0)} + C \cdot \frac{(\nu_1 - \nu_2)^2}{\nu_0}.$$

In particular,

$$\limsup_{t \to \infty} \|\mathbf{u}(t) - \mathbf{v}(t)\| \le C \frac{|\nu_1 - \nu_2|}{\sqrt{\nu_2}}.$$

Proof. We subtract (2.13a) from (2.11a) to get

$$\mathbf{w}_t + B(\mathbf{w}, \mathbf{u}) + B(\mathbf{v}, \mathbf{w}) = (\nu_2 - \nu_1)A\mathbf{u} - \nu_2 A\mathbf{w} - \mu P_{\sigma}(I_h(\mathbf{w}))$$

with $\mathbf{w} = \mathbf{u} - \mathbf{v}$ which, using the identity $B(\mathbf{w}, \mathbf{u}) + B(\mathbf{v}, \mathbf{w}) = B(\mathbf{u}, \mathbf{w}) + B(\mathbf{w}, \mathbf{u}) - B(\mathbf{w}, \mathbf{w})$, can be simplified to

$$\frac{1}{2} \frac{d}{dt} \|\mathbf{w}\|^2 + (B(\mathbf{u}, \mathbf{w}), A\mathbf{w}) + (B(\mathbf{w}, \mathbf{u}), A\mathbf{w}) - (B(\mathbf{w}, \mathbf{w}), A\mathbf{w}) \\
= (\nu_2 - \nu_1)(A\mathbf{u}, A\mathbf{w}) - \nu_2 |A\mathbf{w}|^2 - \mu(P_{\sigma}(I_h(\mathbf{w})), A\mathbf{w}).$$

Then, by (2.9) and (2.10)

$$\frac{1}{2}\frac{d}{dt}\|\mathbf{w}\|^2 - (B(\mathbf{w}, \mathbf{w}), A\mathbf{u}) = (\nu_2 - \nu_1)(A\mathbf{u}, A\mathbf{w})$$
$$-\nu_2|A\mathbf{w}|^2 - \mu(P_{\sigma}(I_h(\mathbf{w})), A\mathbf{w}).$$

Hence,

$$\frac{1}{2}\frac{d}{dt}\|\mathbf{w}\|^2 + \nu_2|A\mathbf{w}|^2 = (B(\mathbf{w}, \mathbf{w}), A\mathbf{u}) + (\nu_2 - \nu_1)(A\mathbf{u}, A\mathbf{w}) - \mu(P_{\sigma}(I_h(\mathbf{w})), A\mathbf{w}).$$

By the Brezis–Gallouet inequality (2.2).

$$|(B(\mathbf{w}, \mathbf{w}), A\mathbf{u})| \le c \|\mathbf{w}\|^2 \left\{ 1 + \log \frac{|A\mathbf{w}|^2}{4\pi^2 \|\mathbf{w}\|^2} \right\} |A\mathbf{u}|.$$

Moreover, since $\mu c_0 h^2 \leq \nu_2$ by assumption, we obtain

$$-\mu(P_{\sigma}(I_{h}(\mathbf{w})), A\mathbf{w}) = \mu(\mathbf{w} - P_{\sigma}(I_{h}(\mathbf{w})), A\mathbf{w}) - \mu \|\mathbf{w}\|^{2}$$

$$\leq \mu |P_{\sigma}(\mathbf{w} - I_{h}(\mathbf{w}))||A\mathbf{w}| - \mu \|\mathbf{w}\|^{2}$$

$$\leq \frac{\mu^{2}c_{0}h^{2}}{2\nu_{2}} \|\mathbf{w}\|^{2} + \frac{\nu_{2}}{2}|A\mathbf{w}|^{2} - \mu \|\mathbf{w}\|^{2}$$

$$\leq \frac{\nu_{2}}{2}|A\mathbf{w}|^{2} - \frac{\mu}{2} \|\mathbf{w}\|^{2}.$$

Using the Cauchy-Schwarz and Young's inequalities, we find

$$(\nu_2 - \nu_1)(A\mathbf{u}, A\mathbf{w}) \le |\nu_2 - \nu_1||A\mathbf{u}||A\mathbf{w}|$$

 $\le \frac{|\nu_2 - \nu_1|^2}{\nu_2}|A\mathbf{u}|^2 + \frac{\nu_2}{4}|A\mathbf{w}|^2.$

Together, the above three inequalities imply that

$$\frac{1}{2} \frac{d}{dt} \|\mathbf{w}\|^{2} + \frac{\nu_{2}}{2} |A\mathbf{w}|^{2}
\leq c \|\mathbf{w}\|^{2} \left(1 + \log \frac{|A\mathbf{w}|}{4\pi^{2} \|\mathbf{w}\|^{2}} \right) |A\mathbf{u}| + \frac{(\nu_{2} - \nu_{1})^{2}}{\nu_{2}} |A\mathbf{u}|^{2}
+ \frac{\nu_{2}}{4} |A\mathbf{w}|^{2} - \frac{\mu}{2} \|\mathbf{w}\|^{2}.$$

Hence,

$$\begin{split} \frac{d}{dt} \|\mathbf{w}\|^2 + \frac{\nu_2}{2} |A\mathbf{w}|^2 + \|\mathbf{w}\|^2 \left[\mu - 2c|A\mathbf{u}| \left(1 + \log \frac{|A\mathbf{w}|^2}{4\pi^2 \|\mathbf{w}\|^2} \right) \right] \\ \leq 2 \frac{(\nu_2 - \nu_1)^2}{\nu_2} |A\mathbf{u}|^2. \end{split}$$

Let

$$\beta = \frac{c|A\mathbf{u}|}{2\pi^2\nu_2} \qquad \text{and} \qquad r = \frac{|A\mathbf{w}|^2}{4\pi^2\|\mathbf{w}\|^2}.$$

Applying Lemma 2.4 (which is applicable since $r \geq 1$ by Poincaré's inequality), we obtain

$$\frac{-c|A\mathbf{u}|}{2\pi^2\nu_2}\log\left(\frac{c|A\mathbf{u}|}{2\pi^2\nu_2}\right) \leq \frac{|A\mathbf{w}|^2}{4\pi^2\|\mathbf{w}\|^2} - \frac{c|A\mathbf{u}|}{2\pi^2\nu_2}\left(1 + \log\frac{|A\mathbf{w}|^2}{4\pi^2\|\mathbf{w}\|^2}\right)$$

which can be simplified to

$$-2c|A\mathbf{u}|\log\left(\frac{c|A\mathbf{u}|}{2\pi^2\nu_2}\right) \le \nu_2 \frac{|A\mathbf{w}|^2}{\|\mathbf{w}\|^2} - 2c|A\mathbf{u}|\left(1 + \log\frac{|A\mathbf{w}|^2}{4\pi^2\|\mathbf{w}\|^2}\right).$$

This implies that

$$\frac{1}{2} \frac{d}{dt} \|\mathbf{w}\|^2 + \|\mathbf{w}\|^2 \left[\mu - 2c|A\mathbf{u}| \log \frac{c|A\mathbf{u}|}{2\pi^2 \nu_2} \right] \le 2 \frac{(\nu_2 - \nu_1)^2}{\nu_2} |A\mathbf{u}|^2.$$

By (2.20),

$$2c \log \frac{c|A\mathbf{u}|}{2\pi^2 \nu_2} \le 2c \log \left(\frac{c}{2\pi^2 \nu_2} \cdot \sqrt{c} 4\pi^2 \nu_1 (1+G)^2\right)$$
$$= 2c \log \left(\frac{2\nu_1 c^{3/2}}{\nu_2}\right) + 4c \log(1+G).$$

Let $J := 2c \log(\frac{2\nu_1 c^{3/2}}{\nu_2}) + 4c \log(1+G)$. Then

$$\frac{d}{dt} \|\mathbf{w}\|^2 + [\mu - J|A\mathbf{u}|] \|\mathbf{w}\|^2 \le 2 \frac{(\nu_2 - \nu_1)^2}{\nu_2} |A\mathbf{u}|^2.$$

Young's inequality implies

$$J|A\mathbf{u}| \le \frac{J^2}{2\mu}|A\mathbf{u}|^2 + \frac{\mu}{2},$$

hence,

$$\frac{d}{dt} \|\mathbf{w}\|^2 + \frac{1}{2} \left[\mu - \frac{J^2}{\mu} |A\mathbf{u}|^2 \right] \|\mathbf{w}\|^2 \le 2 \frac{(\nu_2 - \nu_1)^2}{\nu_2} |A\mathbf{u}|^2.$$

Next, we denote $\alpha(t):=\frac{1}{2}[\mu-\frac{J^2}{\mu}|A\mathbf{u}|^2]$ and let $T:=4\pi^2\nu_1$. Thanks to Theorem 2.2 and the assumption $\mu\geq 12\pi^2\nu_1JG_1$, it follows that

$$\gamma := \liminf_{t \to \infty} \int_{t}^{t+T} \alpha(\tau) d\tau = \frac{\mu}{8\pi^{2}\nu_{1}} - \frac{J^{2}}{2\mu} \left(\liminf_{t \to \infty} \int_{t}^{t+T} |A\mathbf{u}|^{2} d\tau \right)$$

$$\geq \frac{\mu}{8\pi^{2}\nu_{1}} - \frac{J^{2}}{2\mu} \left(16\pi^{2} G_{1}^{2} \nu_{1} \right) > \frac{3}{2} J G_{1} - \frac{2}{3} J G_{1} = \frac{5}{6} J G_{1} > 0.$$

Clearly, it follows that

$$\Gamma := \limsup_{t \to \infty} \int_t^{t+T} \alpha^-(\tau) d\tau < \infty,$$

where $\alpha^{-}(t)$ is defined as in Lemma 2.3.

Choose t_0 sufficiently large so that Theorem 2.2 holds and the inequalities (2.22) and (2.23) hold. Then, we can apply Lemma 2.3 to obtain, for a.e. $t > t_0$,

$$\|\mathbf{w}(t)\|^{2} \leq \|\mathbf{w}(t_{0})\|^{2} \Gamma' e^{-\frac{\gamma}{2T}(t-t_{0})} + \left(\sup_{t \geq t_{0}} \int_{t}^{t+T} 2 \frac{|\nu_{2} - \nu_{1}|^{2}}{\nu_{2}} |A\mathbf{u}(\tau)|^{2} d\tau \right) \Gamma' \frac{e^{\gamma/2}}{e-1},$$

where Γ' is defined in Lemma 2.3. Taking the limit supremum as $t \to 0$ establishes the result.

4. Computational comparison. In the previous section, we showed that the data assimilation algorithm (2.13) can still perform well even when there is an error in the viscosity parameter. In practice, the complexity of small viscosity flows requires more computational resources to accurately simulate, but our simulations in this section indicate that if one has (sparse) measurement data collected on such a flow continuously over a time interval [0,T] it may be possible to construct an accurate computational simulation of the flow over the same time interval using a much larger value for the viscosity, saving computational resources. However, one would still need to use the true viscosity in simulations after time T to accurately predict the behavior of the flow, because we have no data after time T. Hence, in order to more accurately predict the true behavior of the flow, it would be better to somehow recover the true viscosity. We note that our analytical results from the preceding section demonstrate that we have also obtained a lower bound on the viscosity error, $|\nu_2 - \nu_1|$, in terms of the resulting data assimilation error.

The outline of this section is as follows: in section 4.1, we describe the computational setup and choice of data assimilation parameters; in section 4.2, we test the performance of the AOT algorithm without parameter recovery.

- 4.1. Computational setting. All of the following computations were performed on the supercomputer Karst at Indiana University, using *dedalus*, an open source pseudospectral python package, available at http://dedalus-project.org (see [11]). A 512^2 computational resolution was used, with a 3/2 dealiasing factor. A simple explicit/implicit time stepping scheme was used for each simulation, where the linear terms were handled implicitly, and the nonlinear terms explicitly. The spatial domain we consider is $[0, 2\pi]$.
- **4.1.1. Reference solution.** We take our reference solution to be the solution, \mathbf{u}^* , of (2.1) with

$$\nu_1 = 0.001$$

and

$$f = \sum_{9 < |\mathbf{k}| < 11} \widehat{f}_{\mathbf{k}} e^{i\mathbf{k} \cdot \mathbf{x}},$$

and with the initial condition $\mathbf{u}^*(0) = 0$. Each $\hat{f}_{\mathbf{k}}$ is normally distributed, and scaled so that |f| = 1.

We do not have a closed form solution for \mathbf{u}^* so instead we approximate it numerically by solving (2.1) computationally over the time interval [0, 30]. We call the computational approximation we obtain \mathbf{u} , and denote its Fourier transform by $\hat{\mathbf{u}}$. So, for all $t \in [0, 30]$,

$$\mathbf{u}(\mathbf{x},t) = \sum_{|\mathbf{k}| \le 256} \widehat{\mathbf{u}}_{\mathbf{k}}(t) e^{i\mathbf{k} \cdot \mathbf{x}}.$$

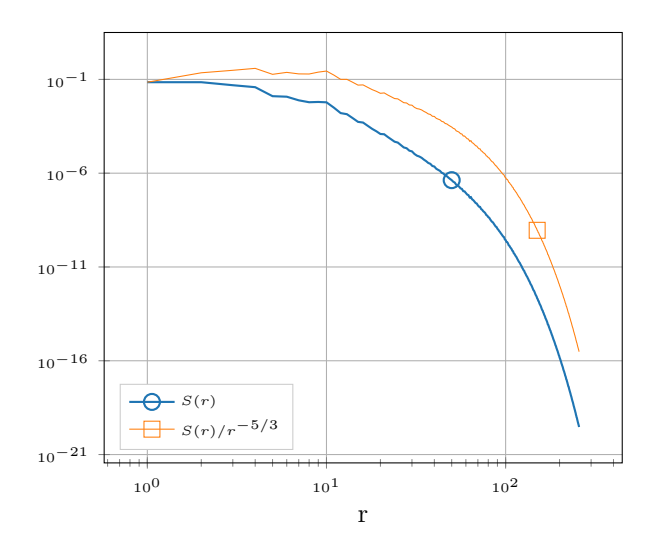


Fig. 1. Spectrum of the computed reference solution over the time interval [20, 30].

Figure 1 shows the spectrum of **u** over the time interval [20, 30], where we define the spectrum, $S:[0,\infty)\to\mathbb{R}$, by

$$S(r) = \frac{1}{10} \int_{20}^{30} \sum_{r - \frac{1}{2} < |\mathbf{k}| \le r + \frac{1}{2}} |\widehat{\mathbf{u}}_{\mathbf{k}}(t)|^2 dt.$$

4.1.2. Data assimilation parameters. In the following numerical experiments, we only consider the case that I_h is the projection onto the low modes, i.e.,

$$I_h(\mathbf{u}) = (\mathbf{x}, t) \mapsto \sum_{|\mathbf{k}| \le \frac{1}{h}} \widehat{\mathbf{u}}_{\mathbf{k}}(t) e^{i\mathbf{k} \cdot \mathbf{x}}.$$

We used a spectral method to compute \mathbf{u} , so we can readily construct $I_h(\mathbf{u})$. In a practical situation, $I_h(\mathbf{u})$ would be given to us and we would have no knowledge of \mathbf{u} ; instead, we use $I_h(\mathbf{u})$ to compute \mathbf{v} with the expectation that $\mathbf{v}(t) \approx \mathbf{u}(t)$ for all t after a time t_0 . In section 4.2 we simulate this situation by computing \mathbf{v} and comparing it to \mathbf{u} .

Before we can compute \mathbf{v} , we will need to choose values for μ and h. The rigorous estimates we have obtained thus far are sufficient conditions, and do not determine the most efficient values of μ and h in practice. Specifically, for the reference solution we have computed, $G_1 = 10^6$, so to satisfy the requirements of Theorem 3.1, we would need $\mu \sim 10^{12}$ and $h \sim 10^{-6}$. To compute $I_h(\mathbf{u})$ with $h = 10^{-6}$, in addition to requiring a large amount of data in practice, would require we increase the computational resolution at least to $200,000^2$.

Fortunately, the algorithm works with much less data, and with much smaller μ . This has been observed when the viscosity is known exactly for the Navier–Stokes equations [29] and for other dissipative systems [2, 18, 19, 32]. In [18] it was shown for the Rayleigh–Bénard equations that analogous rigorous convergence criteria become sharp only as the Prandtl number becomes infinite. In general, a larger Grashof number seems to require a larger μ and a smaller h, as has been observed in the

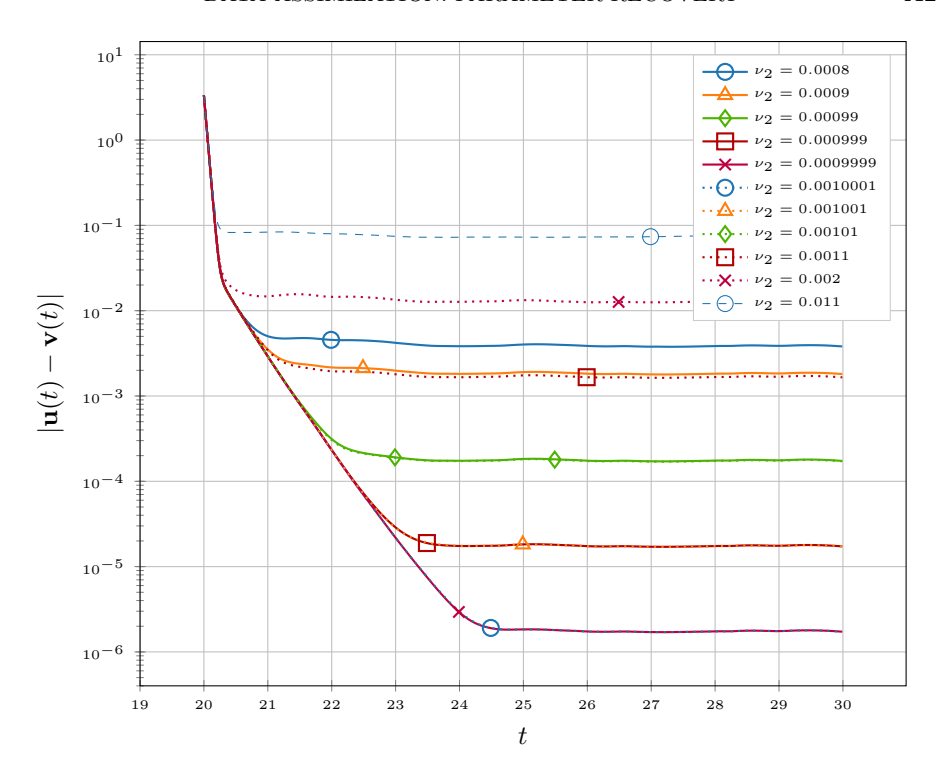


Fig. 2. The evolution of the L^2 error is shown for the solutions of the data assimilation system corresponding to several different values of ν_2 . The minimum L^2 error achieved decreases as the viscosity error decreases.

computational studies mentioned above. However, a comprehensive study of the performance of the algorithms here, or of optimal choices for h or μ , is not within the scope of this paper and will be presented elsewhere. For our purposes, we only need for the algorithm to work for some reasonable choice of μ and h. So, for simplicity, and motivated by the results in [32], we will take

$$\mu = 20, \quad h = \frac{1}{32} = 0.03125.$$

4.2. Subgrid simulations. We are now ready to test the performance of the data assimilation algorithm when $\nu_2 \neq \nu_1$. We compute the solutions of (2.13) corresponding to several values of ν_2 , with percentage error, $|\nu_2 - \nu_1|/\nu_1$, ranging from 1000% to 0.1%. Each solution is computed over the time interval [20, 30] with the initial condition $\mathbf{v}(20) \equiv 0$. Starting the data assimilation simulation at time t = 20 is sufficient in this case to ensure that \mathbf{u} is past a transient (and so is approximating a physical flow), and will be nontrivial at t = 20 (and therefore differs from \mathbf{v} at the start of the simulation).

Figure 2 shows the resulting L^2 error we observed for each simulation compared to \mathbf{u} over the same time interval. We see that for each simulation, after a transient period of fast convergence, the error decreases exponentially at a nearly constant rate before reaching a minimum value. Also, the rates of convergence are the same for each simulation.

5. Parameter recovery. In this section, we construct a rudimentary algorithm to correct the estimated viscosity ν_2 toward the true (but unknown) viscosity ν_1 , using

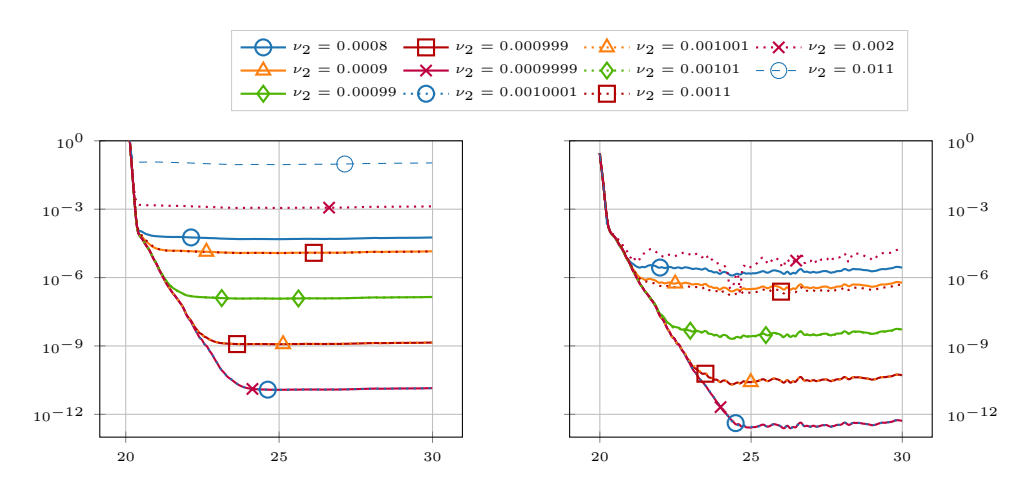


FIG. 3. Shown on the left is $\mu |I_h(\mathbf{v}) - I_h(\mathbf{u})|^2$ versus time for several different values of ν_2 . We see that in each case, $|I_h(\mathbf{v}) - I_h(\mathbf{u})|$ reaches a minimum value, which is smaller for ν_2 closer to ν_1 . On the right is the value of the right-hand side of (5.2) for the same values of ν_2 . We see that the values on the right are negligible compared to the error values on the left.

only the sparse observational data collected from the flow, $I_h(\mathbf{u})$, and the solution of the data assimilation algorithm, \mathbf{v} . We then test the algorithm computationally, demonstrating a full recovery of true behavior of the flow. An analytical proof of the convergence of this algorithm will be the subject of a future work.

We can see in Figure 2 that the error in the viscosity value is directly correlated with the minimum error achieved by the corresponding data assimilation solution. This observation motivates the following: given the data $I_h(\mathbf{u})$, we can compute \mathbf{v} and use the minimum error we observe to estimate the true viscosity, ν_1 .

Although $I_h(\mathbf{u})$ is sufficient to compute \mathbf{v} , we would need to have \mathbf{u} to compute $|\mathbf{u} - \mathbf{v}|$. Fortunately, we see that $|\nu_2 - \nu_1|$ and $|I_h(\mathbf{u}) - I_h(\mathbf{v})|$ are also correlated, as can be seen in Figure 3.

With this in mind, we will now study this correlation, so that, once its nature is established, we can use it to develop an algorithm to estimate ν_1 .

5.1. A posteriori error estimate. The result in Theorem 3.1, in addition to being in terms of the true error (as opposed to the error of only the interpolations of \mathbf{u} and \mathbf{v}), establishes bounds for the data assimilation error in terms of the Grashof number. We are now considering a situation where we have access to \mathbf{v} , and so would like to obtain a sharper estimate on the error by allowing it to be in terms of \mathbf{v} instead of G.

Let $\mathbf{w} = \mathbf{u} - \mathbf{v}$. Subtracting (2.13a) from (2.11a), we obtain

$$\mathbf{w}_t + B(\mathbf{w}, \mathbf{v}) + B(\mathbf{u}, \mathbf{w}) = (\nu_2 - \nu_1)A\mathbf{v} - \nu_1 A\mathbf{w} - \mu P_{\sigma}(I_h(\mathbf{w})).$$

Now, we apply I_h to both sides of this equation and obtain

$$\partial_t I_h(\mathbf{w}) + I_h(B(\mathbf{w}, \mathbf{v}) + B(\mathbf{u}, \mathbf{w}))$$

= $(\nu_2 - \nu_1)I_h(A\mathbf{v}) - \nu_1 I_h(A\mathbf{w}) - \mu I_h(P_\sigma(I_h(\mathbf{w}))).$

Next, we take the inner product with $I_h(\mathbf{w})$ and use the fact that

$$-\mu \langle I_h(P_{\sigma}(I_h(\mathbf{w}))), I_h(\mathbf{w}) \rangle = -\mu |I_h(\mathbf{w})|^2.$$

The result, after rearranging terms, is

(5.1)
$$\frac{1}{2} \frac{d}{dt} |I_h(\mathbf{w})|^2 + (\nu_1 - \nu_2) \langle I_h(A\mathbf{v}), I_h(\mathbf{w}) \rangle + \mu |I_h(\mathbf{w})|^2$$
$$= - \langle I_h(\nu_1 A\mathbf{w} + B(\mathbf{w}, \mathbf{v}) + B(\mathbf{u}, \mathbf{w})), I_h(\mathbf{w}) \rangle.$$

We have observed in each of our simulations that there is a time at which the error $|I_h(\mathbf{w})|$ reaches a minimum value and thereafter remains constant; then $\frac{d}{dt}|I_h(\mathbf{w})| \approx 0$, and the above equation reduces to

(5.2)
$$(\nu_1 - \nu_2) \langle I_h(A\mathbf{v}), I_h(\mathbf{w}) \rangle + \mu |I_h(\mathbf{w})|^2$$

$$= -\langle I_h(\nu_1 A\mathbf{w} + B(\mathbf{w}, \mathbf{v}) + B(\mathbf{u}, \mathbf{w})), I_h(\mathbf{w}) \rangle.$$

Note that all of the terms on the left-hand side of (5.2) except ν_1 are explicitly computable from data observations. However, on the right-hand side, one would need \mathbf{u} to compute $B(\mathbf{w}, \mathbf{v})$ and $B(\mathbf{u}, \mathbf{w})$. Also, although A commutes with the projection onto the low Fourier modes in the periodic setting, A might not commute with other types of interpolation operators I_h , in which case one could not compute $I_h(A\mathbf{w})$ exactly from the observations $I_h(\mathbf{u})$.

However, we note that in terms of units, each of the terms in (5.2) decreases quadratically with \mathbf{w} as $\mathbf{w} \to 0$ (with the exception of $(\nu_1 - \nu_2) \langle I_h(A\mathbf{v}), I_h(\mathbf{w}) \rangle$), but we control μ and have chosen μ large enough that $\mu |I_h(\mathbf{w})|^2$ dominates the terms on the right-hand side, as can be seen in Figure 3. Therefore, we propose an approximation formed by dropping these terms from the equation and, solving (approximately) for ν_1 , thereby obtaining

(5.3)
$$\nu_1 \approx \nu_2 + \mu \frac{|I_h(\mathbf{w})|^2}{\langle I_h(-A\mathbf{v}), I_h(\mathbf{w}) \rangle}.$$

Since each term on the right-hand side now depends only on given or observable quantities, this approximation motivates an iterative scheme for recovering the viscosity. We therefore test (5.3) as a means of recovering ν_1 , using the data from our simulations. We obtain the approximation $\tilde{\nu}_1$ iteratively, using (5.3) for each of the simulations performed in section 4.2 at time t=24, and compare this to ν_1 . The results are shown in Table 1. In each case, (5.3) produces a much better approximation of the true ν_1 , showing at least an 80% improvement. Furthermore, since the algorithm we propose involves changing the viscosity midsimulation, we need to verify it does not in general lead to badly discontinuous behavior, e.g., introducing nonphysical shocks, oscillations, etc. Thus, in a related work [12], we examine the sensitivity of the equations with respect to the viscosity, specifically, we prove local-in-time bounds on solutions to the viscosity-sensitivity equations associated with (2.13) (i.e., bounds on $\frac{\partial \mathbf{u}}{\partial \nu}$ in appropriate spaces).

To avoid waiting until the time derivative of the error becomes negligible, or to include the possibility that the time derivative has nonnegligible oscillations, we can choose to leave the time derivative in (5.1). Let $t > s \ge t_0$. We then integrate (5.1) over the time interval [s, t], to obtain

$$\begin{split} &\frac{1}{2}|I_h(\mathbf{w}(t))|^2 - \frac{1}{2}|I_h(\mathbf{w}(s))|^2 \\ &+ (\nu_1 - \nu_2) \int_s^t \left\langle I_h(A\mathbf{v}(\tau)), I_h(\mathbf{w}(\tau)) \right\rangle d\tau + \mu \int_s^t |I_h(\mathbf{w}(\tau))|^2 d\tau \\ &= - \int_s^t \left\langle I_h((\nu_1 A\mathbf{w} + B(\mathbf{w}, \mathbf{v}) + B(\mathbf{u}, \mathbf{w}))(\tau)), I_h(\mathbf{w}(\tau)) \right\rangle d\tau. \end{split}$$

Table 1

ν_2	$ I_h(\mathbf{w}) ^2$	$\langle I_h(-A\mathbf{v}), I_h(\mathbf{w}) \rangle$	$ ilde{ u}_1$	$ \tilde{\nu}_1 - \nu_1 $	$\frac{ \tilde{\nu}_1 - \nu_1 }{ \nu_2 - \nu_1 }$
0.00080000	1.564e-03	-2.462e-01	9.986e-04	1.381e-06	0.69%
0.00090000	7.786e-04	-1.226e-01	9.988e-04	1.155e-06	1.15%
0.00099000	7.760e-05	-1.223e-02	9.999e-04	1.495e-07	1.49%
0.00099900	7.762e-06	-1.222e-03	1.000e-03	1.423e-08	1.42%
0.00099990	8.309e-07	-1.223e-04	1.000e-03	1.288e-08	12.88%
0.00100010	8.339e-07	1.221e-04	1.000e-03	1.391e-08	13.91%
0.00100100	7.765e-06	1.222e-03	1.000e-03	1.328e-08	1.33%
0.00101000	7.755e-05	1.222e-02	1.000e-03	1.551e-07	1.55%
0.00110000	7.732e-04	1.218e-01	1.002e-03	1.826e-06	1.83%
0.00200000	7.570e-03	1.183e+00	1.031e-03	3.121e-05	3.12%
0.01100000	6.750e-02	9.430e+00	1.336e-03	3.356e-04	3.36%

Then, dropping the terms on the right-hand side as before and solving for ν_1 , we obtain

(5.4)
$$\nu_1 \approx \nu_2 + \frac{\mu \int_s^t |I_h(\mathbf{w}(\tau))|^2 d\tau + \frac{1}{2} |I_h(\mathbf{w}(t))|^2 - \frac{1}{2} |I_h(\mathbf{w}(s))|^2}{\int_s^t \langle I_h(-A\mathbf{v}(\tau)), I_h(\mathbf{w}(\tau)) \rangle d\tau}.$$

5.2. Algorithms. We next use (5.3) and (5.4) to devise algorithms capable of recovering ν_1 using only the data $I_h(\mathbf{u})$ over a time interval $[t_0, T]$. The first algorithm (Algorithm 5.1) utilizes (5.3). Algorithm 5.2 describes a method to recover ν_1 using (5.4) instead of (5.3).

Algorithm 5.1

```
\overline{\text{input } I_h(\mathbf{u})} \text{ on } [t_0, T]
                                                                                                                                                   > available reference solution data
input \nu_2
                                                                                                                                                                        \triangleright an initial estimate for \nu_1
input dt > 0

    time step

input \epsilon > 0

    ▶ tolerance for machine precision

input \delta \in (0,1)

    b tolerance for convergence

t \leftarrow t_0
\mathbf{v}(t_0) \leftarrow 0
 \begin{aligned} \mathbf{w}hile & \left|I_h(\mathbf{u}(t)) - I_h(\mathbf{v}(t))\right| > \epsilon \text{ , AND } t < T \text{ do} \\ \mathbf{compute} & \mathbf{v}(t+dt) \text{ using viscosity } \nu_2 \text{ and feedback } I_h(\mathbf{u}(t)) \\ \mathbf{if} & \left|I_h(\mathbf{u}(t+dt)) - I_h(\mathbf{v}(t+dt))\right| \ge (1-\delta) |I_h(\mathbf{u}(t)) - I_h(\mathbf{v}(t))| \text{ then} \\ \mathbf{if} & \left|I_h(\mathbf{u}(t+dt)) - I_h(\mathbf{v}(t+dt))\right| < |I_h(\mathbf{u}(t_0)) - I_h(\mathbf{v}(t_0))| \text{ then} \end{aligned} 
                         compute \tilde{\nu}_1 using (5.3) at time t+dt
                         t_0 \leftarrow t + dt
                         \nu_2 \leftarrow \tilde{\nu}_1
                        return \nu_2
                 end if
          end if
         t \leftarrow t + dt
end while
return \nu_2
```

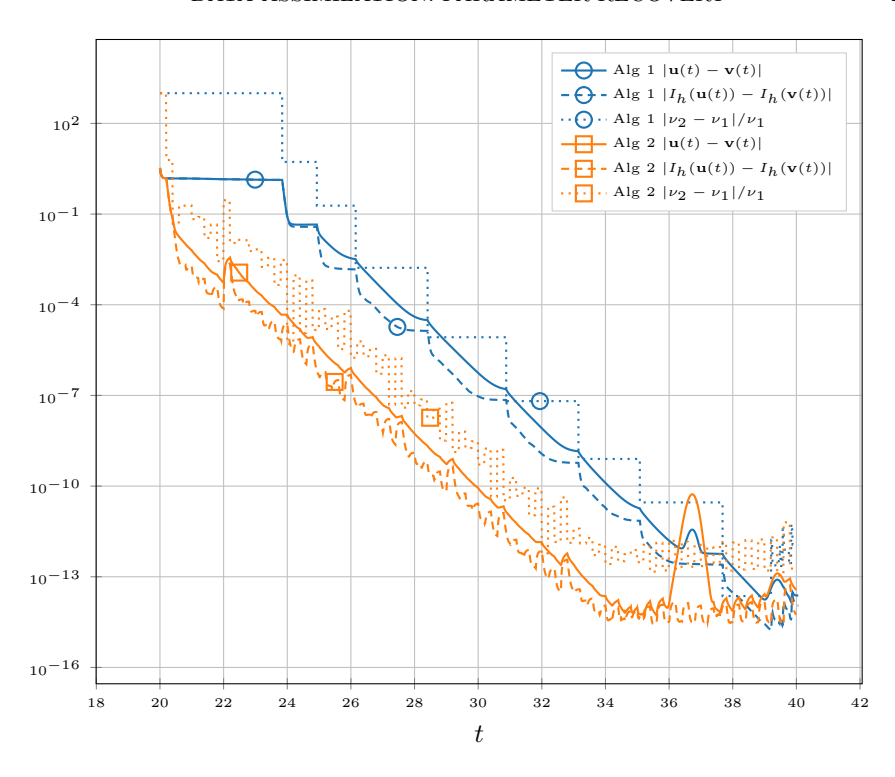


Fig. 4. The evolution of the L^2 error is shown for the solutions of the data assimilation systems corresponding to Algorithms 5.1 and 5.2, as well as that of the relative error in the approximate viscosity. The ν_k are chosen and the equations updated following the procedures outlined in the algorithms.

```
Algorithm 5.2
```

```
input I_h(\mathbf{u}) on [t_0, T]
                                                                                   input \nu_2
                                                                                              \triangleright an initial estimate for \nu_1
input dt > 0
                                                                                                                      input I > 0

    b time to wait before computing time averages

input J > 0
                                                  ▷ length of time interval used to compute time averages
input \epsilon > 0

▷ tolerance for machine precision

\mathbf{v}_0 \leftarrow 0
t \leftarrow t_0
while |I_h(\mathbf{u}(t)) - I_h(\mathbf{v}(t))| > \epsilon, AND t_0 + I + J < T do compute \mathbf{v}(t) on [t_0, t_0 + I + J] using viscosity \nu_2, feedback I_h(\mathbf{u}(t)), IC \mathbf{v}(t_0) = \mathbf{v}_0, and time step
     compute \tilde{\nu}_1 using (5.4) over the time interval [t_0 + I, t_0 + I + J].
     \mathbf{v}_0 \leftarrow \mathbf{v}(t_0 + I + J)
     t_0 \leftarrow t_0 + I + J
     \tilde{\nu_2} \leftarrow \tilde{\nu}_1
end while
return \nu_2
```

6. Conclusion. In this article, we presented and analyzed a new way to recover unknown parameters of a system (in this case, the viscosity), using a CDA approach for the 2D incompressible Navier–Stokes equations. This means that even in the case where the viscosity is unknown and one only has sparse observational data, one may still obtain convergence to the true solution by using the AOT algorithm in combination with the algorithms proposed here. In addition, our new algorithms allow

one to update the viscosity in real time using only observational data, and we showed computationally that the true solution and the true viscosity are recovered to within machine precision, exponentially fast in time. An analytical proof of this will be the subject of a forthcoming work, which will also explore the extension of the algorithm to other physical systems. Furthermore, and as a lead-up to the new algorithms, we proved analytically that in the case of an inaccurately known viscosity, the large-time error produced by the AOT algorithm is controlled by the error in the viscosity.

REFERENCES

- D. A. ALBANEZ, H. J. NUSSENZVEIG LOPES, AND E. S. TITI, Continuous data assimilation for the three-dimensional Navier-Stokes-α model, Asymptot. Anal., 97 (2016), pp. 139–164.
- [2] M. U. ALTAF, E. S. TITI, O. M. KNIO, L. ZHAO, M. F. McCabe, and I. Hoteit, Downscaling the 2D Benard convection equations using continuous data assimilation, Comput. Geosci, 21 (2017), pp. 393–410.
- R. A. Anthes, Data assimilation and initialization of hurricane prediction models, J. Atmos. Sci., 31 (1974), pp. 702–719, https://doi.org/10.1175/1520-0469(1974)031(0702:DAAIOH) 2.0 CO:2
- [4] A. AZOUANI, E. OLSON, AND E. S. TITI, Continuous data assimilation using general interpolant observables, J. Nonlinear Sci., 24 (2014), pp. 277–304, https://doi.org/10.1007/ s00332-013-9189-y.
- [5] L. C. Berselli, T. Iliescu, and W. J. Layton, Mathematics of Large Eddy Simulation of Turbulent Flows, Sci. Comput., Springer, Berlin, 2006.
- [6] H. BESSAIH, E. OLSON, AND E. S. TITI, Continuous data assimilation with stochastically noisy data, Nonlinearity, 28 (2015), pp. 729-753, https://doi.org/10.1088/0951-7715/28/3/729.
- [7] A. BISWAS, C. FOIAS, C. F. MONDAINI, AND E. S. TITI, Downscaling data assimilation algorithm with applications to statistical solutions of the Navier-Stokes equations, Ann. Inst. H. Poincaré Anal. Non Linéaire, 36 (2018), pp. 295-326.
- [8] A. BISWAS AND V. R. MARTINEZ, Higher-order synchronization for a data assimilation algorithm for the 2D Navier-Stokes equations, Nonlinear Anal. Real World Appl., 35 (2017), pp. 132–157, https://doi.org/10.1016/j.nonrwa.2016.10.005.
- [9] D. BLÖMKER, K. LAW, A. M. STUART, AND K. C. ZYGALAKIS, Accuracy and stability of the continuous-time 3DVAR filter for the Navier-Stokes equation, Nonlinearity, 26 (2013), pp. 2193-2219, https://doi.org/10.1088/0951-7715/26/8/2193.
- [10] H. Brezis and T. Gallouet, Nonlinear Schrödinger evolution equations, Nonlinear Anal., 4 (1980), pp. 677–681, https://doi.org/10.1016/0362-546X(80)90068-1.
- [11] K. J. Burns, G. M. Vasil, J. S. Oishi, D. Lecoanet, and B. P. Brown, Dedalus: A Flexible Framework for Numerical Simulations with Spectral methods, preprint, https://arxiv.org/ abs/1905.10388, 2019.
- [12] E. CARLSON, J. HUDSON, AND A. LARIOS, Convergence of Difference Quotient Approximations to Solutions of the Viscosity Sensitivity Equations of the 2D Navier-Stokes Equations and a Continuous Data Assimilation Algorithm, manuscript.
- [13] E. CELIK, E. OLSON, AND E. S. TITI, Spectral filtering of interpolant observables for a discretein-time downscaling data assimilation algorithm, SIAM J. Appl. Dyn. Syst., 18 (2019), pp. 1118–1142, https://doi.org/10.1137/18M1218480.
- [14] P. CONSTANTIN AND C. FOIAS, Navier-Stokes Equations, Chicago Lect. Math., University of Chicago Press, Chicago, IL, 1988.
- [15] R. DALEY, Atmospheric Data Analysis, Cambridge Atmosp. Space Sci. Ser., Cambridge University Press, Cambridge, 1993.
- [16] S. Desamsetti, H. Dasari, S. Langodan, O. Knio, I. Hoteit, and E. S. Titi, Efficient dynamical downscaling of general circulation models using continuous data assimilation, Quart. J. Roy. Meteorol. Soc., 145 (2019), pp. 3175–3194.
- [17] P. C. DI LEONI, A. MAZZINO, AND L. BIFERALE, Inferring flow parameters and turbulent configuration with physics-informed data assimilation and spectral nudging, Phys. Rev. Fluids, 3 (2018), 104604.
- [18] A. FARHAT, N. GLATT-HOLTZ, V. MARTINEZ, S. MCQUARRIE, AND J. P. WHITEHEAD, Data Assimilation in Large-Prandtl Rayleigh—Bénard Convection from Thermal Measurements, preprint, arXiv:1903.01508, 2019.
- [19] A. FARHAT, H. JOHNSTON, M. JOLLY, AND E. S. TITI, Assimilation of nearly turbulent Rayleigh-Bénard flow through vorticity or local circulation measurements: A compu-

- $tational\ study,$ J. Sci. Comput., 77 (2018), pp. 1519–1533, https://doi.org/10.1007/s10915-018-0686-x.
- [20] A. FARHAT, M. S. JOLLY, AND E. S. TITI, Continuous data assimilation for the 2D Bénard convection through velocity measurements alone, Phys. D, 303 (2015), pp. 59–66, https: //doi.org/10.1016/j.physd.2015.03.011.
- [21] A. FARHAT, E. LUNASIN, AND E. S. TITI, Abridged continuous data assimilation for the 2D Navier-Stokes equations utilizing measurements of only one component of the velocity field, J. Math. Fluid Mech., 18 (2016), pp. 1-23.
- [22] A. FARHAT, E. LUNASIN, AND E. S. TITI, Data assimilation algorithm for 3D Bénard convection in porous media employing only temperature measurements, J. Math. Anal. Appl., 438 (2016), pp. 492–506.
- [23] A. FARHAT, E. LUNASIN, AND E. S. TITI, On the Charney conjecture of data assimilation employing temperature measurements alone: The paradigm of 3D planetary geostrophic model, Math. Clim. Weather Forecast., 2 (2016).
- [24] A. FARHAT, E. LUNASIN, AND E. S. TITI, Continuous data assimilation for a 2D Bénard convection system through horizontal velocity measurements alone, J. Nonlinear Sci., 27 (2017), pp. 1065–1087, https://doi.org/10.1007/s00332-017-9360-y.
- [25] C. Foias, O. Manley, R. Rosa, and R. Temam, Navier-Stokes Equations and Turbulence, Encyclopedia Math. Appl. 83, Cambridge University Press, Cambridge, 2001.
- [26] C. FOIAS, C. F. MONDAINI, AND E. S. TITI, A discrete data assimilation scheme for the solutions of the two-dimensional Navier-Stokes equations and their statistics, SIAM J. Appl. Dyn. Syst., 15 (2016), pp. 2109-2142, https://doi.org/10.1137/16M1076526.
- [27] K. FOYASH, M. S. DZHOLLI, R. KRAVCHENKO, AND E. S. TITI, A unified approach to the construction of defining forms for a two-dimensional system of Navier-Stokes equations: The case of general interpolating operators, Uspekhi Mat. Nauk, 69 (2014), pp. 177-200.
- [28] B. GARCÍA-ARCHILLA, J. NOVO, AND E. S. TITI, Uniform in Time Error Estimates for a Finite Element Method Applied to a Downscaling Data Assimilation Algorithm for the Navier-Stokes Equations, preprint, arXiv:1807.08735, 2018.
- [29] M. GESHO, E. OLSON, AND E. S. TITI, A computational study of a data assimilation algorithm for the two-dimensional Navier-Stokes equations, Commun. Comput. Phys., 19 (2016), pp. 1094-1110.
- [30] N. GLATT-HOLTZ, I. KUKAVICA, V. VICOL, AND M. ZIANE, Existence and regularity of invariant measures for the three dimensional stochastic primitive equations, J. Math. Phys., 55 (2014), 051504, https://doi.org/10.1063/1.4875104.
- [31] J. E. HOKE AND R. A. ANTHES, The initialization of numerical models by a dynamic-initialization technique, Monthly Weather Rev., 104 (1976), pp. 1551–1556.
- [32] J. Hudson and M. Jolly, Numerical efficacy study of data assimilation for the 2D magnetohydrodynamic equations, J. Comput. Dyn., 6 (2019), pp. 131–145, https://doi.org/10. 3934/jcd.2019006.
- [33] H. A. IBDAH, C. F. MONDAINI, AND E. S. TITI, Fully discrete numerical schemes of a data assimilation algorithm: uniform-in-time error estimates, IMA J. Numer. Anal., to appear https://doi.org/10.1093/imanum/drz043.
- [34] M. S. Jolly, V. R. Martinez, E. J. Olson, and E. S. Titi, Continuous data assimilation with blurred-in-time measurements of the surface quasi-geostrophic equation, Chinese Ann. Math. Ser. B, 40 (2019), pp. 721–764, https://doi.org/10.1007/s11401-019-0158-0.
- [35] M. S. JOLLY, V. R. MARTINEZ, AND E. S. TITI, A data assimilation algorithm for the subcritical surface quasi-geostrophic equation, Adv. Nonlinear Stud., 17 (2017), pp. 167–192, https: //doi.org/10.1515/ans-2016-6019.
- [36] M. S. JOLLY, T. SADIGOV, AND E. S. TITI, A determining form for the damped driven nonlinear Schrödinger equation—Fourier modes case, J. Differential Equations, 258 (2015), pp. 2711– 2744, https://doi.org/10.1016/j.jde.2014.12.023.
- [37] D. A. Jones and E. S. Titi, Determining finite volume elements for the 2D Navier– Stokes equations, Phys. D, 60 (1992), pp. 165–174, https://doi.org/10.1016/0167-2789(92) 90233-D.
- [38] R. E. KALMAN, A new approach to linear filtering and prediction problems, J. Basic Eng., 82 (1960), pp. 35–45.
- [39] E. KALNAY, Atmospheric Modeling, Data Assimilation and Predictability, Cambridge University Press, New York, 2003.
- [40] S. LAKSHMIVARAHAN AND J. M. LEWIS, Nudging methods: A critical overview, in Data Assimilation for Atmospheric, Oceanic and Hydrologic Applications, Vol. II, Springer, Berlin, 2013, pp. 27–57.

- [41] A. Larios and Y. Pei, Approximate continuous data assimilation of the 2D Navier–Stokes equations via the Voigt-regularization with observable data, Evol. Equ. Control Theory, to appear.
- [42] A. LARIOS AND Y. Pei, Nonlinear continuous data assimilation, preprint, arXiv:1703.03546, 2017.
- [43] A. LARIOS, L. G. REBHOLZ, AND C. ZERFAS, Global in time stability and accuracy of IMEX-FEM data assimilation schemes for Navier-Stokes equations, Comput. Methods Appl. Mech. Engrg., https://doi.org/10.1016/j.cma.2018.09.004, (2018).
- [44] A. LARIOS AND C. VICTOR, Continuous data assimilation with a moving cluster of data points for a reaction diffusion equation: A computational study, Commun. Comput. Phys., (2019), to appear.
- [45] K. LAW, A. STUART, AND K. ZYGALAKIS, A Mathematical Introduction to Data Assimilation, Texts Appl. Math. 62, Springer, Cham, Switzerland, 2015.
- [46] P. C. DI LEONI, A. MAZZINO, AND L. BIFERALE, Synchronization to Big-Data: Nudging the Navier-Stokes Equations for Data Assimilation of Turbulent Flows, preprint, arXiv:1905.05860, 2019.
- [47] M. LESIEUR, O. METAIS, AND P. COMTE, Large-Eddy Simulations of Turbulence, Cambridge University Press, New York, 2005, https://doi.org/10.1017/CBO9780511755507.
- [48] J. LEWIS AND S. LAKSHMIVARAHAN, Sasakiś pivotal contribution: Calculus of variations applied to weather map analysis, Monthly Weather Rev., 136 (2008), pp. 3553-3567.
- [49] E. Lunasin and E. S. Titi, Finite determining parameters feedback control for distributed nonlinear dissipative systems—a computational study, Evol. Equ. Control Theory, 6 (2017), pp. 535–557, https://doi.org/10.3934/eect.2017027.
- [50] P. A. MARKOWICH, E. S. TITI, AND S. TRABELSI, Continuous data assimilation for the three-dimensional Brinkman-Forchheimer-extended Darcy model, Nonlinearity, 29 (2016), pp. 1292–1328, https://doi.org/10.1088/0951-7715/29/4/1292.
- [51] C. F. Mondaini and E. S. Titi, Uniform-in-time error estimates for the postprocessing Galerkin method applied to a data assimilation algorithm, SIAM J. Numer. Anal., 56 (2018), pp. 78–110, https://doi.org/10.1137/16M110962X.
- [52] Y. Pei, Continuous Data Assimilation for the 3D Primitive Equations of the Ocean, Comm. Pure Appl. Anal., 18 (2019), pp. 643–661, https://doi.org/10.3934/cpaa.2019032.
- [53] L. G. Rebholz and C. Zerfas, Simple and efficient continuous data assimilation of evolution equations via algebraic nudging, 2018, https://arxiv.org/abs/arXiv:1810.03512.
- [54] J. C. ROBINSON, Infinite-Dimensional Dynamical Systems, Cambridge Texts Appl. Math., Cambridge University Press, Cambridge, 2001.
- [55] P. SAGAUT, Large Eddy Simulation for Incompressible Flows, 3rd ed., Scientific Comput., Springer-Verlag, Berlin, 2006.
- [56] R. TEMAM, Navier-Stokes Equations and Nonlinear Functional Analysis, 2nd ed., CBMS-NSF Regional Conf. Ser. in Appl. Math. 66, SIAM, Philadelphia, 1995.
- [57] R. Temam, Navier-Stokes Equations: Theory and Numerical Analysis, AMS Chelsea Publishing, Providence, RI, 2001.
- [58] C. Zerfas, L. G. Rebholz, M. Schneier, and T. Iliescu, Continuous data assimilation reduced order models of fluid flow, Comput. Methods Appl. Mech. Engrg., 357 (2019), 112596, https://doi.org/10.1016/j.cma.2019.112596.